Discotic liquid crystals of transition metal complexes 51[†]: Synthesis and mesomorphism of flat-pumpkin-shaped phthalocyanine-fullerene dyads

Miho Yoshioka[a], Kazuchika Ohta[a*], Yohei Miwa[b], Shoichi Kutsumizu[b] and Mikio Yasutake[c]

[a] *Smart Material Science and Technology, Department of Bioscience and Textile Technology, Interdisciplinary, Graduate School of Science and Technology, Shinshu University, 1-15-1 Tokida, Ueda, 386-8567, Japan.*

[b] *Department of Chemistry, Faculty of Engineering, Gifu University, Gifu 501-1193, Japan.*

[c] *Comprehensive Analysis Center for Science, Saitama University, 255 Shimo-okubo, Sakura-ku, Saitama 338-8570, Japan.*

ABSTRACT: We have synthesised a novel type of donor-acceptor liquid crystalline material, phthalocyanine-fullerene (Pc-C_{60}) dyad, [*m*, *p*, *m'*-$(C_{14}O)_3PhO]_6PcCu$-C_{60} (**7**), and the Pc precursors, [*m*, *p*, *m'*-$(C_{14}O)_3PhO]_6PcCu$-OFBA (**6**) and [*m*, *p*, *m'*-$(C_{14}O)_3PhO]_6PcCu$-OH (**5**), and established their mesomorphism by using a polarizing optical microscope, a differential scanning calorimeter and a small angle X-ray diffractometer. Very interestingly, their corresponding previous parent Pc derivative, [*m*, *p*, *m'*-$(C_{14}O)_3PhO]_8PcCu$ (**4**), shows a very wide temperature region *ca.* 90°C of a bicontinuous Cub(Pn3m) mesophase, whereas the present children Pc precursors (**5** and **6**) and Pc-C_{60} dyad **7** show not the Cub mesophase but a Col_{ho} mesophase. It is also noteworthy that the staking distance in the Col_{ho} mesophase of the Pc-C_{60} dyad **7** was a very big value of ca. 9.1 Å, which is the biggest in discotic liquid crystals to our best knowledge. It may be originated from the biggest excluded volume caused by thermal fluctuation of peripheral long alkoxy chains at *m*, *m'*-positions. The excluded volume caused by thermal fluctuation of the peripheral long chains is so big that the molecular shape of the Pc derivative **4** and the Pc-C_{60} dyad **7** very resembles a flat pumpkin.

KEYWORDS: Discotic liquid crystal, phthalocyanine, fullerene, dyad, cubic mesophase, columnar mesophase

INTRODUCTION

Discotic liquid crystals generally consist of a rigid central core and several flexible long chains in the periphery. Since the discovery in 1977 [1], various kinds of discotic liquid crystalline compounds have been synthesized and investigated [2-5]. It is well known in the most discotic liquid crystals that disk-like π-conjugated central cores pile up face-to-face by their $\pi-\pi$ interaction to form one-dimensional columnar structures, which show hexagonal columnar (Col$_h$), tetragonal columnar (Col$_{tet}$), rectangular columnar (Col$_r$) mesophases and others (Fig. 1). Moreover, charge carriers can so effectively transfer through these columns by hopping conduction that discotic liquid crystals are expected application as electronic materials to solar cell and so on [5-7]. Driving force of columnar formation in disk-like molecules is intermolecular interaction of the central cores. This intermolecular interaction strength effects on the resultant columnar structures [8-10]. Hence, it is very interesting that the intermolecular interaction among the central cores may be controlled by the peripheral substituents.

Recently, we have synthesized the phthalocyanine (Pc) derivatives peripherally substituted by eight, sixteen, and twenty four long chains, (m-C$_{14}$OPhO)$_8$PcCu (**1**), (p-C$_{14}$OPhO)$_8$PcCu (**2**), [m, p-(C$_{14}$O)$_2$PhO]$_8$PcCu (**3**) and [m, p, m'-(C$_{14}$O)$_3$PhO]$_8$PcCu (**4**), respectively, as shown in Fig. 1, and investigated effect of the position and number of the peripheral long chains on their mesomorphism [11, 12]. As a result, we found that their mesomorphism largely altered with the number of peripheral long chains. As shown in Table 1, the derivatives, **1** and **2**, substituted by eight long chains show only Col$_h$ mesophases; the derivative **3** substituted by sixteen long chains show very rich columnar mesophases and a very narrow temperature region of a bicontinuous cubic mesophase Cub(Pn3m); the derivative **4** substituted by twenty four long chains shows the bicontinuous cubic mesophase Cub(Pn3m) in a wide temperature region of *ca.* 90°C. It is noteworthy that the cubic mesophase temperature region becomes wider with increasing the number of peripheral long chains.

In these Pc derivatives, the central core disk-like parts tend to form one-dimensional columns by their π-π interaction, so that the columns may branch to form not a globular micelle cubic phase but a bicontinuous cubic phase (Fig. 1). However, there have been a very few reports on discotic compounds exhibiting a thermotropic cubic mesophase [11-25] in comparison with the rod-like compounds. Therefore, cubic mesophases exhibited by discotic compounds are very fascinating to investigate relationship between the molecular structures and the mesophase structures.

On the other hand, if an excellent electron donor of Pc-based liquid crystal can be covalently connected with an excellent electron acceptor of fullerene (C$_{60}$), the resultant dyad liquid crystal has both properties of donor and acceptor, and the boundary between donors and acceptors may be controllable by alignment of the dyads in the columnar mesophase. Therefore, various liquid crystalline Pc-C$_{60}$ dyads have been synthesized as electronic materials for applications to solar cells and etc. [26-38]. It is noteworthy that the mesomorphism of the resultant Pc-C$_{60}$ dyads are strongly influenced by that of the parent Pc compounds [37, 38].

In this study, we focus on the [m, p, m'-(C$_{14}$O)$_3$PhO]$_8$PcCu derivative (**4**) substituted by twenty four long alkoxy chains that shows a bicontinuous Cub(Pn3m) mesophase in which disk-like Pc molecules pile up face-to-face to form three-dimensionally branched columns [12]. If a corresponding [m, p, m'-(C$_{14}$O)$_3$PhO]$_6$PcCu-C$_{60}$ dyad (**7** in Scheme 1) substituted by eighteen long alkoxy chains would show the bicontinuous Cub mesophase in a wide temperature region as well as the parent Pc derivative **4**, the Pc-C$_{60}$ dyad might pile up face-to-face to form three-dimensionally branched columns [12]. Therefore, donor-acceptor dyads showing a bicontinuous Cub mesophase enable the charge carriers transfer all the direction through the bicontinuous columns. In this case, we do not need homeotropic alignment of the columns between two glass plates [19-22], so that we may fabricate high efficiency of organic thin film solar cells by using the bicontinuous Cub mesophase of Pc-C$_{60}$ dyad. Accordingly, in this study we have synthesized the Pc-C$_{60}$ dyad

7 derived from the parent Pc compound **4** showing a wide temperature range of bicontinuous Cub mesophase, in order to investigate mesomorphism of the dyad.

EXPERIMENTAL

Synthesis

Scheme 1 shows the synthetic route for Pc-C_{60} dyads, [m, p, m'-$(C_{14}O)_3$PhO]$_6$PcCu-C_{60} (**7**). 4-(10-Hydroxy-decyloxy)phthalonitrile (**8**) and 4,5-bis(3,4,5-tris-tetradecyloxy-phenoxy)-1,2-dicyanobenzene (**9**) were synthesized by previously reported methods [12, 37]. The Pc precursors, [m, p, m'-$(C_{14}O)_3$PhO]$_6$PcCu-OH (**5**), was synthesized from these two different phthalonitriles **8** and **9** in a molecular ratio of 3:1. The terminal OH group in **5** was esterified with p-formyl benzoic acid by Steglich reaction to afford [m, p, m'-$(C_{14}O)_3$PhO]$_6$PcCu-OFBA (**6**). Finally, the target Pc-C_{60} dyad, [m, p, m'-$(C_{14}O)_3$PhO]$_6$PcCu-C_{60} (**7**), was synthesized from **6** with N-methylglycine and fullerene by Prato reaction. These synthetic methods for the Pc derivatives (**5-7**) were a little bit modified our previously reported ones [37]. We describe the detailed procedures in the followings.

[m, p, m'-(C₁₄O)₃PhO]₆PcCu-OH (5)

A mixture of 4-decyloxyphthalonitrile (**8**) (0.0316 g, 0.105 mmol), 4,5-bis-(3,4,5-tris-tetradecyloxyphenoxy)-phthalonitrile (**9**) (0.500 g, 0.315 mmol), 1-hexanol (15ml), $CuCl_2$ (0.0440 g, 0.327 mmol) and DBU (5 drops) was refluxed under nitrogen atmosphere for 24 h. After cooling to r.t., methanol was poured into the reaction mixture to precipitate the target compound. The methanolic layer was filtrated and then the resulting precipitate was washed with methanol, ethanol and acetone, successively. The residue was purified by column chromatography (silica gel, chloroform, Rf = 0.82) and recrystallisation from ethyl acetate to afford 0.172 g of green solid. Yield = 32.0 %.

Elemental analysis data: See Table 2.

MALDI-TOF mass data: See Table 3.

UV-vis spectral data: See Table 4.

[m, p, m'-(C₁₄O)₃PhO]₆PcCu-OFBA (6)

A mixture of [m, p, m'-$(C_{14}O)_3$PhO]$_6$PcCu-OH (**5**) (0.1178 g、0.0299 mmol), p-formyl benzoic acid (0.1107 g、0.737 mmol) and dry CH_2Cl_2 (20 ml) was stirred at 50°C under a nitrogen atmosphere for 15min. Then, N, N'-dicyclohexylcarbodiimide (0.0805 g, 0.390 mmol) and N, N-dimethyl-4-aminopyridine (0.0360 g、0.295 mmol) were added to the mixture and it was stirred at 50°C under a nitrogen atmosphere for 14.5 h. After cooling to r.t., methanol was poured into the reaction mixture to precipitate the target compound. The methanolic layer was filtrated and then the resulting precipitate was washed with methanol, ethanol and acetone, successively. The residue was purified by recrystallization from ethyl acetate and then column chromatography (silica gel, chloroform, Rf = 0.95) to afford 0.0985 g of green solid. Yield = 62.7 %.

Elemental analysis data: See Table 2.

MALDI-TOF mass data: See Table 3.

UV-vis spectral data: See Table 4.

[m, p, m'-(C₁₄O)₃PhO]₆PcCu-C₆₀ (7)

A mixture of [m, p, m'-$(C_{14}O)_3$PhO]$_6$PcCu-OFBA (**6**) (0.0774 g、0.0147 mmol), fullerene (0.0215 mg、0.0298 mmol), dry toluene (20 ml) and N-methylglycine (0.0119 mg、0.134 mmol) was refluxed under nitrogen atmosphere for 12 h. After cooling to r.t., the solvent was evaporated under reduced pressure. The residue was extracted with chloroform and washed with water. The organic layer was dried over Na_2SO_4 and evaporated *in vacuum*. The crude product was purified by flash chromatography to remove the unreacted purple fullerene (silica gel, n-hexane; R_f = 1.0).

After the removal, the desired green product adsorbed on the gel was collected by using chloroform as the eluent. Further purification was carried out by using HPLC (Japan Analytical Industry Co. Ltd: LC-918) to afford 0.0324 g of green solid. Yield = 36.7 %.

MALDI-TOF mass data: See Table 3.

UV-vis spectral data: See Table 4.

Measurements

The Pc derivatives synthesized here were identified with an elemental analyzer (Perkin-Elmer elemental analyzer 2400), a MALDI-TOF mass spectrometer (AutoflexIII-2S) and an electronic absorption spectrometer (HITACHI U-4100 spectrophotometer). The elemental analysis data and MALDI-TOF mass spectral data are summarized in Tables 2 and 3, respectively. Each of the electronic absorption spectra of all the Pc derivatives is summarized in Table 4. Phase transition behaviour of the present compounds was observed with a polarizing optical microscope (Nikon ECLIPSE E600 POL) equipped with a Mettler FP82HT hot stage and a Mettler FP-90 Central Processor, and a Shimadzu DSC-50 differential scanning calorimeter. The mesophases were identified by using a small angle X-ray diffractometer (Bruker Mac SAXS System) equipped with a temperature-variable sample holder adopted a Mettler FP82HT hot stage, which measurable range is from 3.0 Å to 100 Å and the temperature range is from r.t. to $375^{o}C$ [37]. In addition to this X-ray diffractometer, another small angle X-ray diffractometer (Rigaku **Nano Viewer**) was also used for the Pc-C_{60} dyad [m, p, m'-$(C_{14}O)_3PhO]_6PcCu$-C_{60} (**7**).

RESULTS AND DISCUSSION

Synthesis

As can be seen from the data of elemental analysis and MALDI-TOF mass spectra in Tables 2 and 3, the observed values of Pc derivatives, [m, p, m'-$(C_{14}O)_3PhO]_6PcCu$-OH (**5**) and [m, p, m'-$(C_{14}O)_3PhO]_6PcCu$-OFBA (**6**), satisfactorily agree with the calculated values. On the other hand, the Pc-C_{60} dyad, [m, p, m'-$(C_{14}O)_3PhO]_6PcCu$-C_{60} (**7**), gave less carbon content by several percentage than the calculated value, due to imperfect combustion. This is a well-known characteristic of less flammable Pc derivatives, which have been reported in the previous papers [35-39]. Therefore, the elemental analysis data were omitted in Table 2. However, as can be seen from the MALDI-TOFF mass spectra of the dyad **7** in Figure S1, no other detectable derivatives are present without the target dyad **7** and the fragment reduced fullerene from the dyad **7** by laser irradiation during the measurement. Thus, the MALDI-TOFF mass and electronic spectra listed in Tables 3 and 4 gave satisfactory evidence of successful synthesis of the target Pc-C_{60} dyad (**7**).

Phase transition behaviour

Table 5 summarizes phase transition behaviour of the novel Pc precursors, **5** and **6**, and the corresponding Pc-C_{60} dyad **7**. As can be seen from this table, the freshly prepared (virgin) sample of [m, p, m'-$(C_{14}O)_3PhO]_6PcCu$-OH (**5**) was a mixture of two crystalline polymorphs, K_1 and K_2, which, on heating, transformed into an unidentified mesophase, M_x, at $31.3^{o}C$ and $39.5^{o}C$, respectively; on further heating, this M_x mesophase cleared into isotropic liquid at $63.5^{o}C$. In the same manner, the virgin sample of [m, p, m'-$(C_{14}O)_3PhO]_6PcCu$-OFBA (**6**) was also a mixture of two crystalline polymorphs, K_1 and K_2, which, on heating, transformed into an unidentified mesophase, M_x, at $30.4^{o}C$ and $41.9^{o}C$, respectively; on further heating, this M_x mesophase cleared into isotropic liquid at $62.4^{o}C$. On the other hand, the virgin sample of [m, p, m'-$(C_{14}O)_3PhO]_6PcCu$-C_{60} (**7**) showed a crystalline phase (K_1) at r.t. On heating, it transformed into a hexagonal ordered columnar (Col_{ho}) mesophase at $22.2^{o}C$ and then the Col_{ho} mesophase relaxed into another crystalline

4

phase (K_2). When this K_2 phase was heated, it transformed into the Col_{ho} mesophase at 33.6°C and, on further heating, this Col_{ho} mesophase cleared into isotropic liquid at 54.9°C.

Fig. 2 illustrates free energy versus temperature (G-T) diagrams for these three derivatives **5-7**. Routes 1 and 2 for the Pc derivatives **5** and **6** show the phase transition sequences starting from crystalline polymorphs K_1 and K_2 by indicating with dotted and open arrows, respectively. As can be seen from these G-T diagrams, the melting point from crystalline phase to M_x mesophase depends on the route. Route 1 gives the lower m.p. (31.3°C for **5**; 30.4°C for **6**). On the other hand, the clearing point from M_x to isotropic liquid (I.L.) does not depend on the route. In contrast with these Pc derivatives **5** and **6**, the Pc-C_{60} dyad **7** follows only one route as illustrated in the G-T diagram. When the virgin sate of Crystal K_1 is heated, it melts into Col_{ho} at 22.2°C and the resultant Col_{ho} mesophase resolidifies into Crystal K_2 by relaxation; on further heating, Crystal K_2 melts again into Col_{ho} at 33.6°C and then the Col_{ho} mesophase clears into I.L. at 54.9°C.

Thus, the complicated phase transition behaviour of the present compounds **5-7** can be rationally explained by using these G-T diagrams.

X-ray mesophase structure analysis

In order to precisely identify the mesophases, we carried out temperature-dependent X-ray mesophase structure analysis. Fig.s 3 and 4 show X-ray diffraction patterns of the Pc derivatives (**5** and **6**) and the Pc-C_{60} dyad (**7**), respectively. In Table 6 are listed all the X-ray data.

As can be seen from Fig. 3, each of the Pc derivatives, [*m*, *p*, *m'*-$(C_{14}O)_3PhO]_6$PcCu-OH (**5**) and [*m*, *p*, *m'*-$(C_{14}O)_3PhO]_6$PcCu-OFBA (**6**), showed only one sharp peak in the low angle region and two broad peaks in the wide angle region for the mesophase. Therefore, we could not identify these mesophases from only one peak in the low angle region, so that we call them as an unidentified mesophase, M_x. However, if the M_x mesophase in the Pc derivative **5** would be assumed as a Col_{ho} mesophase, the lattice constant could be calculated as a = 37.8 Å from Peak 1. Two broad peaks, 2 and 3, could be assigned as the stacking distance (h = *ca.* 9.4 Å) and average distance among the molten alkoxy chains (# = ca. 4.6 Å), respectively. Similarly, if the M_x mesophase in the Pc derivative 6 would be also assumed as a Col_{ho} mesophase, we could calculate to get a = 36.8 Å, h = *ca.* 9.4 Å and # = ca. 4.6 Å. These calculations are consistent with the results of a = 34.6 Å, h = *ca.* 9.1 Å and # = ca. 4 Å for the well-established Col_{ho} mesophase in the Pc-C_{60} dyad (**7**) mentioned in the followings.

As can be seen from Fig. 4, the Pc-C_{60} dyad, [*m*, *p*, *m'*-$(C_{14}O)_3PhO]_6$PcCu-C_{60} (**7**) at 45.7°C gave two big sharp peaks, 1 and 2, and one small broad peak 3 in the low angle region, and two very broad peaks, 4 and 5, in the wide angle region. At first we could not detect Peak 3 (See Fig. 4 [A] and [C]). After annealing at 45.7°C for 9 hours, we could detect Peak 3 at last (See Fig. 4 [B]). Peaks 2 and 3 could be assignment to (100) and (110) reflections from a 2D hexagonal lattice having a lattice constant a = 34.6 Å, by using Reciprocal Lattice Calculation Method [40]. Broad peaks 4 and 5 could be assigned a sacking distance (h = *ca.* 9.1 Å) and the average distance among molten alkoxy chains (# = ca. 4.6 Å), respectively. Peak 1 denoted as Peak H appeared in the very low angle region only for this Pc-C_{60} dyad **7**. Peak H did not appear for the Pc precursors **5** and **6**. Furthermore, this peak could not be assigned to any reflection in all the 2D lattices known up to date. Recently, we found the same Peak H in the other Pc-C_{60} dyads, and established from the detailed XRD studies that Peak H can be assigned as a helical pitch of C_{60} moieties around the Pc columns [37, 38]. Hence, the present Peak H was also assigned as a helical pitch of C_{60} moieties.

Columnar structures

Very interestingly, the parent Pc derivative **4** shows a very wide temperature region, *ca.* 90°C, of a Cub mesophase (Table 1), whereas the corresponding child Pc-C_{60} dyad **7** does not exhibit a Cub mesophase (Table 5), contrary to our expectation. Moreover, the children Pc precursors, **5** and **6**, also show not a Cub mesophase but a Col_{ho} mesophase.

Thus, the mesomorphism of neither the Pc precursors (**5** and **6**) nor the Pc-C_{60} dyad (**7**) depends on the mesmorphism of the parent Pc derivative (**4**). It is totally different from the tendency reported in previous examples [37, 38] that the mesmorphism of all the children of the Pc precursors and the Pc-C_{60} dyad is the same as the mesomorphism of the parent Pc derivative. We thought that it might be attributable to the number of peripheral long alkoxy chains.

The Pc parent derivative **4** is substituted by 24 long alkoxy chains in the periphery. On the other hand, the corresponding child Pc-C_{60} dyad **7** is substituted by 18 long alkoxy chains in the periphery. The number of long alkoxy chains in the child Pc-C_{60} dyad **7** is less by 6 than that in the parent Pc derivative **4**. Therefore, this difference may greatly affect disappearance of the Cub mesophase. In order to prepare the Pc-C_{60} dyad, the number of long alkoxy chains in the parent Pc derivative was reduced by 6. As a result, it may reduce the excluded volume caused by thermal fluctuation of the peripheral long alkoxy chains. Furthermore, in the Pc-C_{60} dyad **7**, aggregation power among the fullerene moieties is added to their intermolecular interaction. Accordingly, the Pc-C_{60} dyad **7** may form not branched columns but straight columns to show a Col_{ho} mesophase.

It is also noteworthy in the present X-ray data that the stacking distance in the Col_{ho} mesophase of the Pc-C_{60} dyad **7** was a big value of *ca.* 9.1 Å (Table 6). Up to date, a considerable number of phthalocyanine-based discotic liquid crystals have been synthesized [4], and their stacking distances are generally observed in a range of 3.5-5 Å, although they depend on the number of peripheral long chains and the kind of substituents [12, 15, 41]. Hence, the stacking distance *ca.* 9.1 Å of the Pc-C_{60} dyad is extraordinarily big. However, this stacking distance can be rationally proven as a proper value from Z value calculation [40].

The number (Z) of molecules in a lattice can be calculated from this stacking distance (h = 9.1 Å) and the lattice constant of 2D hexagonal lattice (a = 34.6 Å) listed in Table 6. When ρ, V, N and M are density of mesophase, volume of unite lattice, Avogadro's number and molecular weight, respectively, Z value can be obtained from following equation:

$$Z = (\rho VN)/M = \{\rho \, [\, a^2 \text{ x h x } \sin(120^o)]\, N\}/M$$
$$= [1.0(g/cm^3) \text{ x } (34.6 \text{x} 10^{-8} \text{ cm})^2 \text{ x } (9.1 \text{x} 10^{-8} cm) \text{ x } 0.866 \text{ x } 6.02 \text{ x } 10^{23}(/mol)]/6003.42(g/mol)$$
$$= 0.95$$
$$\approx 1$$

The calculated value Z≈1 is the same as the theoretical number of molecules in a 2D hexagonal lattice: Z = 1.0. Therefore, this big stacking distance h = 9.1 Å is a rationally proper value. The stacking distance h = 9.1 Å is the biggest in discotic liquid crystals, so far as we know. It may be originated from the biggest excluded volume caused by thermal fluctuation of the peripheral long alkoxy chains at the *m*, *m'*-positions. Since two adjacent phenoxy groups cannot freely rotate by their steric hindrance, the phenyl planes are almost perpendicular to the central phthalocyanine (Pc) plane. Therefore, the long alkoxy chains at the *m*, *m'*-positions of phenoxy group are not in the Pc plane; the thermal fluctuation of these long alkoxy chains made very big excluded volume, which may widen the interdisk distance to become such a big stacking distance. It is unfortunately unfavourable for solar cell fabrication that the present Col_{ho} mesophase having such a wide stacking distance might not function as a semiconductor since no overlap of the π-systems exists.

Fig. 5 schematically illustrates the columnar structures in the Cub and Col_{ho} mesophases of the previous parent Pc derivative **4** and the present child Pc- Pc-C_{60} dyad **7**. In this figure, black disks, curves, big open circles and small balls represent Pc disks, long alkoxy chains, excluded volume caused by thermal fluctuation of these chains, and fullerene moieties, respectively. As can be seen from this illustration, the excluded volume (open circles) caused by thermal fluctuation of the peripheral teradecyloxy chains is so big that it resembles pulp of a pumpkin. Hence, the shape of the Pc derivative **4** and the Pc-C_{60} dyad **7** very resembles a flat pumpkin.

6

CONCLUSION

We have synthesised a novel type of donor-acceptor liquid crystalline material, phthalocyanine-fullerene (Pc-C_{60}) dyad, [m, p, m'-($C_{14}O)_3PhO]_6PcCu$-C_{60} (**7**), and the Pc precursors, [m, p, m'-($C_{14}O)_3PhO]_6PcCu$-OFBA (**6**) and [m, p, m'-($C_{14}O)_3PhO]_6PcCu$-OH (**5**), and established their mesomorphism by using a polarizing optical microscope, a differential scanning calorimeter and small angle X-ray diffractometers. Very interestingly, their corresponding previous parent Pc derivative, [m, p, m'-($C_{14}O)_3PhO]_8PcCu$ (**4**), shows a very wide temperature region *ca.* 90°C of a bicontinuous Cub(Pn3m) mesophase, whereas the present children Pc precursors (**5** and **6**) and Pc-C_{60} dyad **7** show not the Cub mesophase but a Col$_{ho}$ mesophase. It is totally different from the previously known tendency that mesomorphism of all the children Pc precursors and Pc-C_{60} dyad is the same as that of the corresponding parent Pc derivative. It may be attributable to the reduction of the number of peripheral long alkoxy chains by 6 from the parent (**4**: 24) to the children (**5~7**: 18). The number reduction may cause the reduction of excluded volume of the peripheral long alkoxy chains to show not a Cub mesophase but a Col$_{ho}$ mesophase. It is also noteworthy that the staking distance in the Col$_{ho}$ mesophase of the Pc-C_{60} dyad **7** was a very big value of ca. 9.1 Å, which is the biggest in discotic liquid crystals, to our best knowledge. It may be originated from the biggest excluded volume caused by thermal fluctuation of peripheral long alkoxy chains at m, m'-positions. It is very interesting that although both of parent Pc derivative **4** and child Pc-C_{60} dyad **7** have almost the same "flat-pumpkin-shape", they show different mesophases of a bicontinuous Cub mesophase and a Col$_{ho}$ mesophase, respectively.

Thus, we revealed that a small reduction of the number of peripheral long chains considerably changes their mesomorphism irrespective of almost the same molecular shapes between the parent Pc derivative and the child Pc-C_{60} dyad. It is very useful for us to further design liquid crystals of donor-acceptor dyads.

REFERENCES

1. Chandrasekhar S, Sadashiva BK and Suresh KA. *Pramana* 1977; **9**: 471-480.

2. Sandeep K. *Liq. Cryst.* 2004; **31**: 1037-1059.

3. Sandeep K. *Chem. Soc. Rev.* 2006; **35**: 83–109.

4. Ohta K, Nguyen-Tran HD, Tauchi L, Kanai Y, Megumi T and Takagi Y. *Handbook of Porphyrin Science* 2011; 12: 1-120.

5. Adam D, Schuhmacher P, Simmerer J, Haussling L, Siemensmeyer K, Etzbach KH, Ringsdorf H and Haarer D. *Nature* 1994; **371**: 141-143.

6. Borden N, Bushby RJ, Clements J and Monaghar B. *Phys. Rev. B* 1995; **52**: 274-280.

7. Ban K, Nishizawa K, Ohta K, van de Craats AM, Warman JM, Yamamoto I and Shirai H. *J. Mater. Chem.* 2001; **11**: 321-331.

8. Herwig P, Kayser CW, Müllen K and Spiess HW. *Adv. Muter.* 1996; **8**: 510-513.

9. Kumar S, Naidu JJ and Rao DSS. *J. Mater. Chem.* 2002; **12**: 1335-1341.

10. Gearba RI, Lehmann M, Levin J, Ivanov DA, Koch MHJ, Barberá J, Debije MG, Piris J and Geerts YH. *Adv. Mater.* 2003; **15**: 1614-1618.

11. Ichihara M, Suzuki A, Hatsusaka K and Ohta K. *J. Porphyrins Phthalocyanines* 2007; **11**: 503-512.

12. Ichihara M, Suzuki A, Hatsusaka K and Ohta K. *Liq. Cryst.* 2007; **34**: 555-567.

13. Kohne B, Praefcke K, Billard J. *Z. Naturfor. B: Anorg. Chem., Org. Chem.* 1986; **41B**; 1036-44.

14. Billard J, Zimmermann H, Poupko R and Luz Z. *J. Phys. France* 1989; **50**: 539-357.

15. Hatsusaka K, Ohta K, Yamamoto I and Shirai H. *J. Mater. Chem*. 2001; **11**: 423-433.

16. Hatsusaka K, Kimura M, Ohta K. *Bull. Chem. Soc. Jpn.* 2003; **76**: 781-787.

17. Mukai H, Hatsusaka K, Ohta K. *J. Porphyrins Phthalocyanines* 2007; 11: 846-856.

18. Alam MA, Motoyanagi J, Yamamoto Y, Fukushima T, Kim J, Kato K, Takata M, Saeki A, Seki S, Tagawa S and Aida T. *J. Am. Chem. Soc.* 2009; **131**: 17722-17723.

19. Mukai H, Yokokawa M, Hatsusaka K, Ohta K. *J. Porphyrins Phthalocyanines* 2009; **13**: 70-76.

20. Mukai H, Yokokawa M, Hatsusaka K, Ohta K. *Liq. Cryst.* 2010, **37**: 13-21.

21. Mori A, Yamamoto E, Kubo K, Ujiie S, Baumeister U and Tichierske C. *Liq. Cryst.* 2010; **37**: 1059-1065.

22. Mukai H, Yokokawa M, Ichihara M, Hatsusaka K and Ohta K. *J. Porphyrins Phthalocyanines* 2010; **14**: 188-197.

23. Ichikawa T, Yoshio M, Hamasaki A, Kagimoto J, Ohno H and Kato T. *J. Am. Chem. Soc.* 2011; **133**: 2163-2169.

24. Debnath S, Srour HF, Donnio B, Fourmigue M and Camerel F. *RSC Adv.* 2012; **2**: 4453-4462.

25. Zhang B, Wang J, Yu ZQ, Yang S, Shi AC and Chen EQ. *J. Mater. Chem. C*, 2014; **2**: 5168-5175.

26. Guldi DM, Zilbermann I, Gouloumis A, Va´zquez P and Torres T. *J. Phys. Chem. B* 2004; **108**: 18485-18494.

27. Uchida S, Kude Y, Nishikitani Y and Ota (= Ohta) K. *Jpn. Kokai Tokkyo Koho.* JP 2008214227(A)-2008-09-18 (Priority number: JP2007060604; Submission Date: 2007-03-09).

28. de la Escosura A, Martınez-Dıaz MV, Barbera J and Torres T. *J. Org. Chem*., 2008; **73**: 1475-1480.

29. Ota (= Ohta) K. *Jpn. Kokai Tokkyo Koho*, JP2011132180(A)-2011-07-07 (Priority number: JP20090293501; Submission Date: 2009-12-24).

30. Geerts YH, Debever O, Amato C and Sergeyev S. *Beilstein J. Org. Chem.* 2009; **5**: 1-9.

31. Torres T, Guldi DM, Bottari G and de la Torre G. *Chem. Rev.*, 2010; **110**: 6768-6816.

32. de Miguel G, Wielopolski M, Schuster DI, Fazio MA, Lee OP, Haley CK, Ortiz AL, Echegoyen L, Clark T and Guldi DM. *J. Am. Chem. Soc.,* 2011; **133**: 13036–13054.

33. Ince M, Martinez-Diaz MV, Barbera J and Torres T. *J. Mater. Chem.* 2011; **21**: 1531-1536.

34. Hayashi H, Nihashi W, Umeyama T, Matano Y, Seki S, Shimizu Y and Imahori H. *J. Am. Chem. Soc.* 2011; **133**: 10736–10739.

35. Kamei T, Kato T, Itoh E and Ohta K. *J. Porphyrins Phthalocyanines* 2012; 16: 1261–1275.

36. Shimizu M, Tauchi L, Nakagaki T, Ishikawa A, Itoh E and Ohta K. *J. Porphyrins Phthalocyanines* 2013; **17**: 264-282.

37. Tauchi L, Nakagaki T, Shimizu M, Itoh E, Yasutake M and Ohta K. *J. Porphyrins Phthalocyanines* 2013; 17: 1080-1093.

38. Ishikawa A, Ono K, Ohta K, Yasutake M, Ichikawa M and Itoh E. *J. Porphyrins Phthalocyanines* 2014; **18**: 366-379.

39. van der Pol JF, Neeleman E, van Miltenburg JC, Zwikker JW, Nolte RJM and Drenth W. *Macromolecules* 1990; **23**: 155–162.

40. Ohta K. *"Dimensionality and Hierarchy of Liquid Crystalline Phases: X-ray Structural Analysis of the Dimensional Assemblies"*, Shinshu University Institutional Repository, submitted on 11 May, 2013; http://hdl.handle.net/10091/17016; Ohta K. *"Identification of discotic mesophases by X-ray structure analysis,"* in *"Introduction to Experiments in Liquid Crystal Science (Ekisho Kagaku Jikken Nyumon [in Japanese]),"* ed., Japanese Liquid Crystal Society, Chapter 2-(3), pp. 11-21, Sigma Shuppan, Tokyo, 2007; ISBN-13: 978-4915666490.

41. Igarashi K, Sato H, Yama Y, Ichihara M, Itoh E and Ohta K. *J. Porphyrins Phthalocyanines* 2012; **16**: 1148-1181.
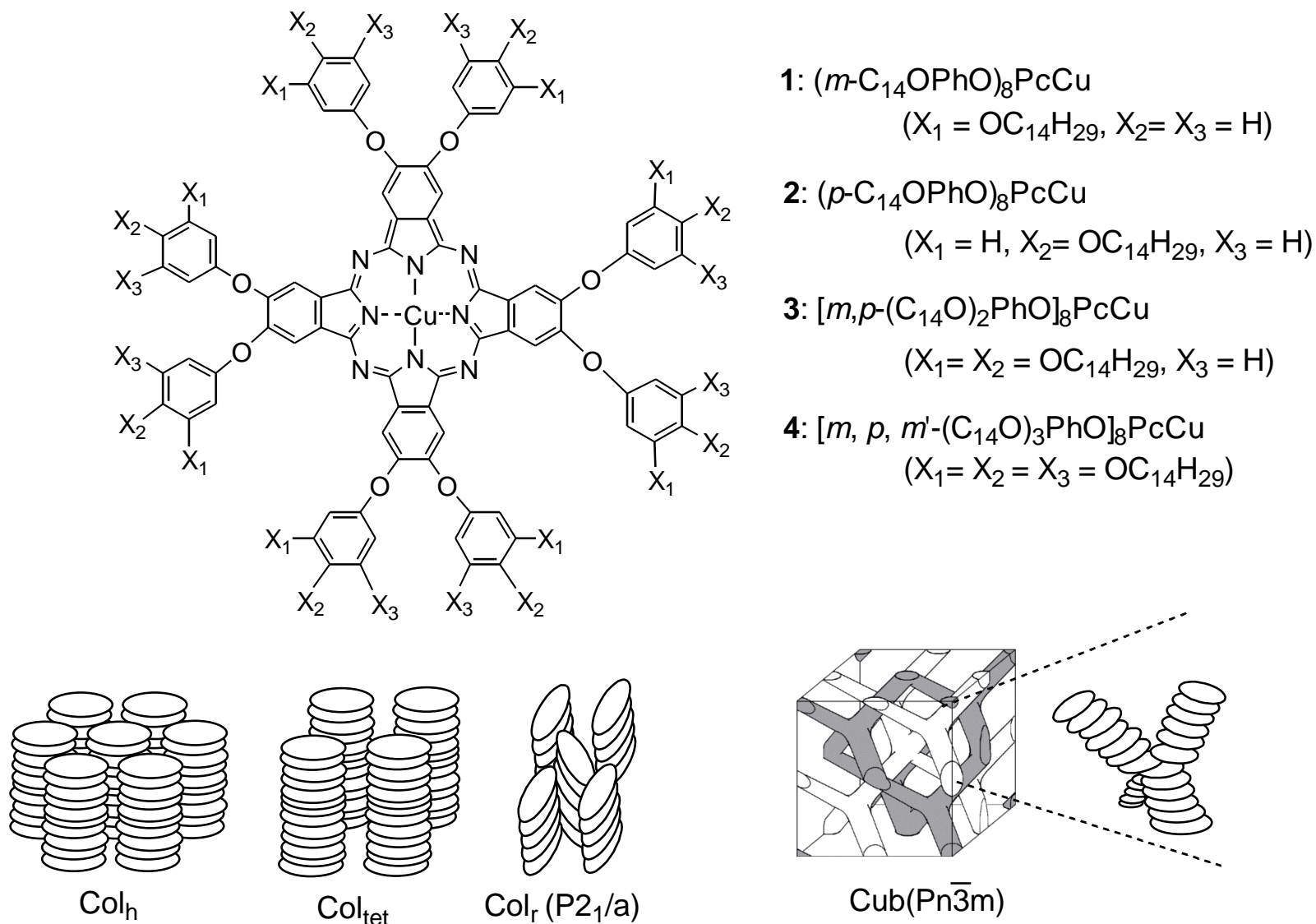
1: (m-C$_{14}$OPhO)$_8$PcCu
    (X$_1$ = OC$_{14}$H$_{29}$, X$_2$= X$_3$ = H)

2: (p-C$_{14}$OPhO)$_8$PcCu
    (X$_1$ = H, X$_2$= OC$_{14}$H$_{29}$, X$_3$ = H)

3: [m,p-(C$_{14}$O)$_2$PhO]$_8$PcCu
    (X$_1$= X$_2$ = OC$_{14}$H$_{29}$, X$_3$ = H)

4: [m, p, m'-(C$_{14}$O)$_3$PhO]$_8$PcCu
    (X$_1$= X$_2$ = X$_3$ = OC$_{14}$H$_{29}$)

Col$_h$ Col$_{tet}$ Col$_r$ (P2$_1$/a)   Cub(Pn$\bar{3}$m)
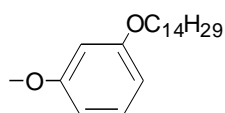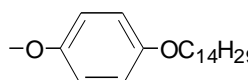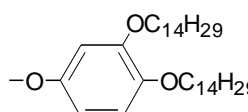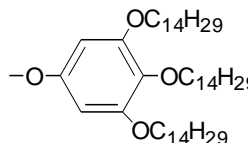
Figure 1. Our previous phthalocyanine compounds, **1-4**, and their columnar structures. Ref. [11, 12].

9

Table 1. Phase transition temperatures and enthalpy changes of our previous phthalocyanine compound, $(m\text{-}C_{14}OPhO)_8PcCu$ (**1**), $(p\text{-}C_{14}OPhO)_8PcCu$ (**2**) and $[m, p\text{-}(C_{14}O)_2PhO]_8PcCu$ (**3**) and $[m, p, m'\text{-}(C_{14}O)_3PhO]_8PcCu$ (**4**).

Compound	Phase	$\xrightarrow{\begin{array}{c}T/\,^oC\\ [\Delta H/\,kJ\,mol^{-1}]\end{array}}$	Phase

1: $(m\text{-}C_{14}OPhO)_8PcCu$

$OC_{14}H_{29}$

$-O-$

$Col_{hd} \xrightarrow[\;]{\begin{array}{c}169.0\\ [22.0]\end{array}} I.L.$

$Col_{ho} \xrightarrow[\;]{\begin{array}{c}169.6\\ [25.5]\end{array}}$

2: $(p\text{-}C_{14}OPhO)_8PcCu$

$-O-\!\!\!\!\bigcirc\!\!\!\!-OC_{14}H_{29}$

$K_{1v} \xrightarrow{\begin{array}{c}88.0\\ [4.62]\end{array}} K_2 \underset{\;}{\overset{\begin{array}{c}113.9\\ [111.2]\end{array}}{\rightleftharpoons}} Col_{hd} \overset{\begin{array}{c}292.3\\ [5.47]\end{array}}{\rightleftharpoons} I.L.$

3: $[m,p\text{-}(C_{14}O)_2PhO]_8PcCu$

$OC_{14}H_{29}$

$-O-\!\!\!\!\bigcirc$

$OC_{14}H_{29}$

$X_v \rightleftharpoons^{ca.\ 20\text{-}90} Col_{hd} \underset{\;}{\overset{\begin{array}{c}111.2\\ [16.1]\end{array}}{\rightleftharpoons}} \begin{array}{c}Col_{rd}\\ (P2_1/a)\end{array} \underset{\;}{\overset{\begin{array}{c}125.6\\ [62.1]\end{array}}{\rightleftharpoons}} Col_{tet.d} \xrightarrow{slow} \begin{array}{c}Cub\\ (Pn\bar{3}m)\end{array} \overset{\begin{array}{c}180.9\\ [3.44]\end{array}}{\rightleftharpoons} I.L.$

169.5

175.5 $\searrow$ I.L.

4: $[m,p,m'\text{-}(C_{14}O)_3PhO]_8PcCu$

$OC_{14}H_{29}$

$-O-\!\!\!\!\bigcirc\!\!\!\!-OC_{14}H_{29}$

$OC_{14}H_{29}$

[275]

$K \underset{\;}{\overset{36.8}{\rightleftharpoons}} \begin{array}{c}Col_r\\ (P2m)\end{array} \underset{\;}{\overset{45.9}{\rightleftharpoons}} Y \xrightarrow{\begin{array}{c}59.6\\ [2.26]\end{array}} \begin{array}{c}Cub\\ (Pn\bar{3}m)\end{array} \overset{\begin{array}{c}144.8\\ [4.88]\end{array}}{\rightleftharpoons} I.L.$

Phase nomenclature: X = unidentified mesophase, Y = unidentified mesophase, K = crystal, Col_{ho} = hexagonal ordered columnar mesophase, Col_{hd} = hexagonal disordered columnar mesophase, Col_{rd} = rectangular disordered columnar mesophase, Cub = cubic phase, $Col_{tet.d}$ = tetragonal disordered columnar mesopahse I.L. = isotropic liquid and v = virgin state. Ref. [11, 12].
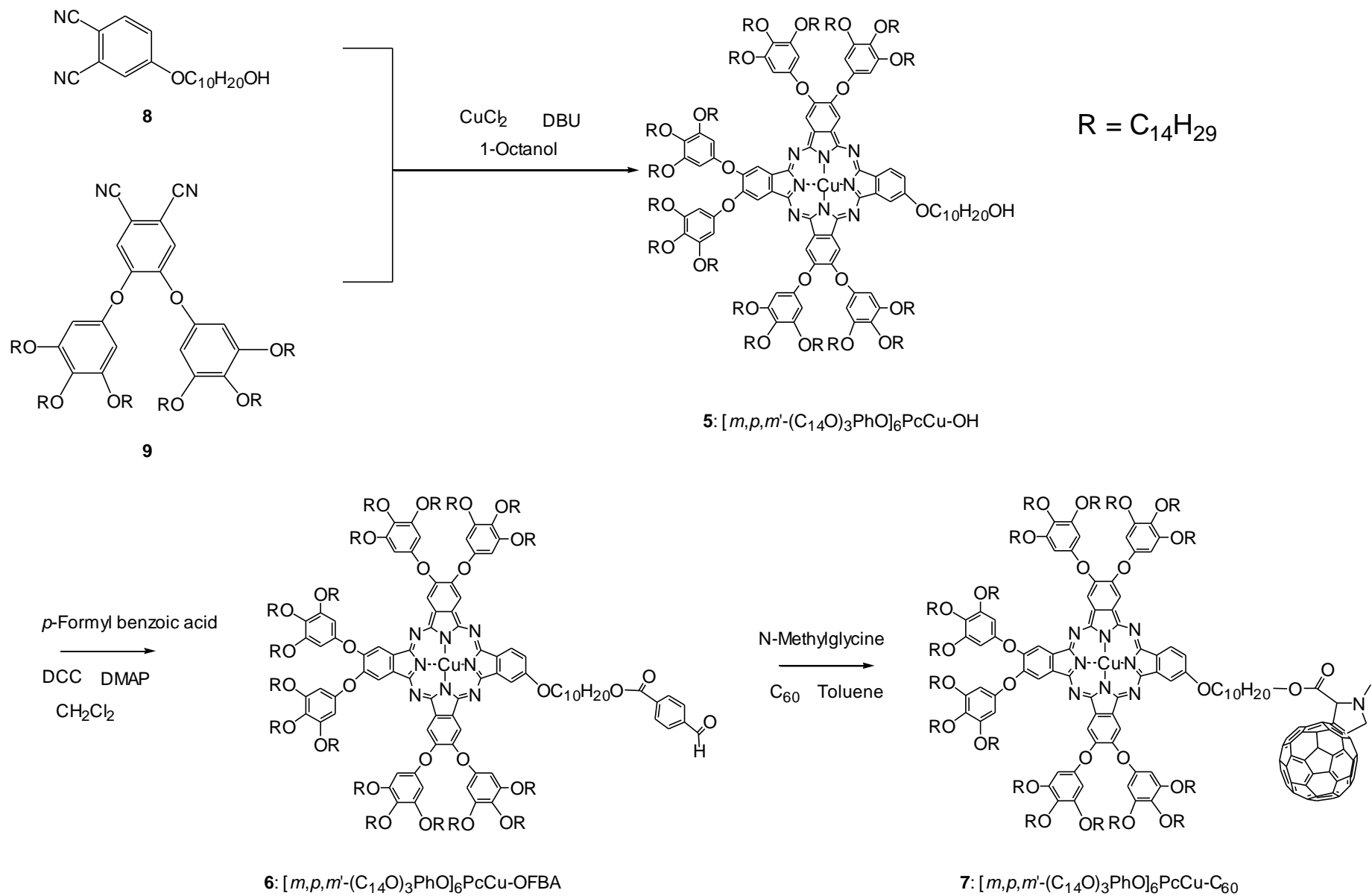
Scheme1. Synthetic route of novel phthalocyanine-fullerene dyad, [(C$_{14}$O)$_3$PhO]$_6$PcCu-C$_{60}$ (**7**). DBU = 1,8-diazabicyclo[5,4,0]-7-undecene.

R = C$_{14}$H$_{29}$

8

9

5: [m,p,m'-(C$_{14}$O)$_3$PhO]$_6$PcCu-OH

6: [m,p,m'-(C$_{14}$O)$_3$PhO]$_6$PcCu-OFBA

7: [m,p,m'-(C$_{14}$O)$_3$PhO]$_6$PcCu-C$_{60}$

CuCl$_2$ DBU
1-Octanol

p-Formyl benzoic acid

DCC DMAP

CH$_2$Cl$_2$

N-Methylglycine

C$_{60}$ Toluene

Table 2. Yields and elemental analysis data of [m, p, m'-$(C_{14}O)_3$PhO]$_6$PcCu-OH (**5**), [m, p, m'-$(C_{14}O)_3$PhO]$_6$PcCu-OFBA (**6**) and [m, p, m'-$(C_{14}O)_3$PhO]$_6$PcCu-C_{60} (**7**).

Compound	Yield (%)	Mol. formula (Mol. wt)	Elemental analysis; found(%) (calc. %)		
			C	H	N
5: [m, p, m'-$(C_{14}O)_3$PhO]$_6$PcCu-OH	32.0	$C_{330}H_{564}N_8O_{26}Cu$ (5123.59)	77.36 (77.85)	11.10 (11.46)	2.19 (2.14)
6: [m, p, m'-$(C_{14}O)_3$PhO]$_6$PcCu-OFBA	62.7	$C_{338}H_{568}N_8O_{28}Cu$ (5255.71)	77.24 (77.57)	10.89 (11.06)	2.13 (1.93)
7: [m, p, m'-$(C_{14}O)_3$PhO]$_6$PcCu-C_{60}	36.7	$C_{400}H_{573}N_9O_{27}Cu$ (6003.42)	-	-	-

Table 3. MALDI-TOF mass spectral data of $[m, p, m'-(C_{14}O)_3PhO]_6PcCu-OH$ (**5**), $[m, p, m'-(C_{14}O)_3PhO]_6PcCu-OFBA$ (**6**) and $[m, p, m'-(C_{14}O)_3PhO]_6PcCu-C_{60}$ (**7**).

Compound	Mol. formula (Exact Mass)	Mass Spectra
5: $[m, p, m'-(C_{14}O)_3PhO]_6PcCu-OH$	$C_{330}H_{564}N_8O_{26}Cu$ (5119.25)	5120.62
6: $[m, p, m'-(C_{14}O)_3PhO]_6PcCu-OFBA$	$C_{338}H_{568}N_8O_{28}Cu$ (5251.27)	5252.69
7: $[m, p, m'-(C_{14}O)_3PhO]_6PcCu-C_{60}$	$C_{152}H_{192}N_8O_{24}Cu$ (5998.31)	5999.40 5279.05*

* = M^+ - 720

Table 4. UV-vis spectral data in chloroform of of [*m, p, m'*-(C$_{14}$O)$_3$PhO]$_6$PcCu-OH (**5**), [*m, p, m'*-(C$_{14}$O)$_3$PhO]$_6$PcCu-OFBA (**6**) and [*m, p, m'*-(C$_{14}$O)$_3$PhO]$_6$PcCu-C$_{60}$ (**7**)

Compound	Concentration[#] (X10^{-5}mol/l)	λ_{max} (nm) (logε)						
		C$_{60}$ Peak	Soret-band			Q-band		
5: [*m, p, m'*-(C$_{14}$O)$_3$PhO]$_6$PcCu-OH	0.995		292.2(4.71)	340.0(4.84)	*ca.*400(4.36)	615.3(4.56)	653.4(4.53)	684.8(5.27)
6: [*m, p, m'*-(C$_{14}$O)$_3$PhO]$_6$PcCu-OFBA	1.01		292.2(4.74)	340.4(4.87)	*ca.*400(4.39)	615.9(4.60)	651.4(4.54)	684.8(5.30)
7: [*m, p, m'*-(C$_{14}$O)$_3$PhO]$_6$PcCu-C$_{60}$	0.999	253.5(5.14)	288.9(4.97)	339.7(4.96)	*ca.*400(4.48)	617.3(4.59)	650.7(4.59)	684.8(5.18)

#: In chloroform

Table 5. Phase transition temperatures of $[m, p, m\text{'-}(C_{14}O)_3PhO]_6PcCu\text{-}OH$ (**5**), $[m, p, m\text{'-}(C_{14}O)_3PhO]_6PcCu\text{-}OFBA$ (**6**) and $[m, p, m\text{'-}(C_{14}O)_3PhO]_6PcCu\text{-}C_{60}$ (**7**).

Compound	Phase $\xrightarrow{\;T(^{o}C)\,[\,\Delta H\,(kJmol^{-1})\,]\;}$ Phase $\rightsquigarrow$ relaxation

5: $[m, p, m\text{'-}(C_{14}O)_3PhO]_6PcCu\text{-}OH$

$K_{1v} \xrightarrow{\;31.3\;} M_x \underset{}{\overset{63.5\;[8.96]}{\rightleftharpoons}} \text{I.L.}$

$K_{2v} \xrightarrow{\;39.5\;} M_x$

6: $[m, p, m\text{'-}(C_{14}O)_3PhO]_6PcCu\text{-}OFBA$

$K_{1v} \xrightarrow{\;30.4\;} M_x \underset{}{\overset{62.4\;[4.32]}{\rightleftharpoons}} \text{I.L.}$

$K_{2v} \xrightarrow{\;41.9\;} M_x$

7: $[m, p, m\text{'-}(C_{14}O)_3PhO]_6PcCu\text{-}C_{60}$

$K_{1v} \xrightarrow{\;22.2\;[7.96]\;} Col_{ho} \rightsquigarrow K_2 \xrightarrow{\;33.6\;[67.1]\;} Col_{ho} \underset{}{\overset{54.9\;[6.44]}{\rightleftharpoons}} \text{I.L.}$

Phase nomenclature : K= crystal, Col_{ho} = hexagonal ordered columnar, M_x = unidentified columnar mesophase, I.L. = isotropic liquid and v = virgin state.
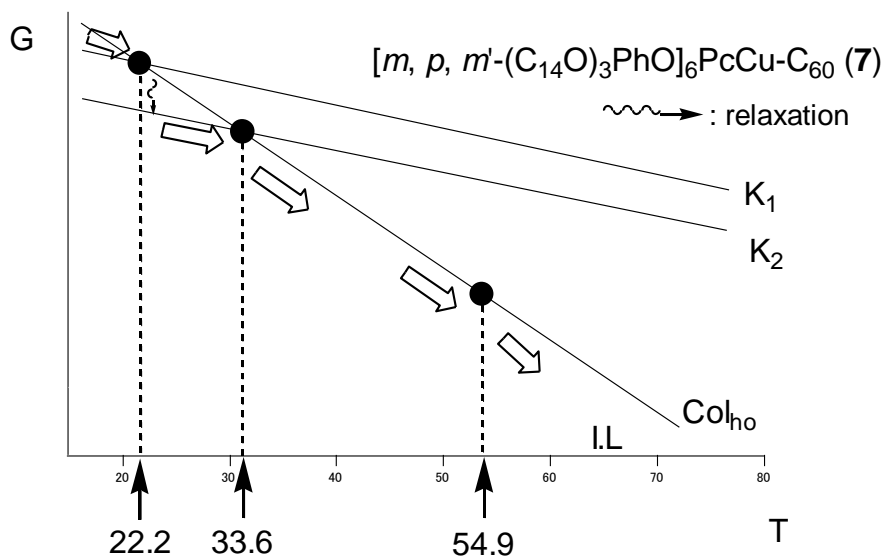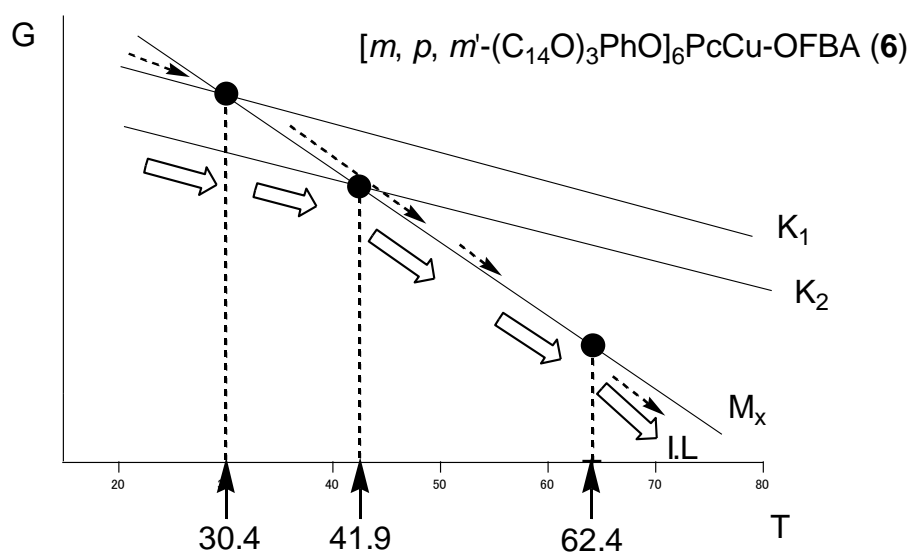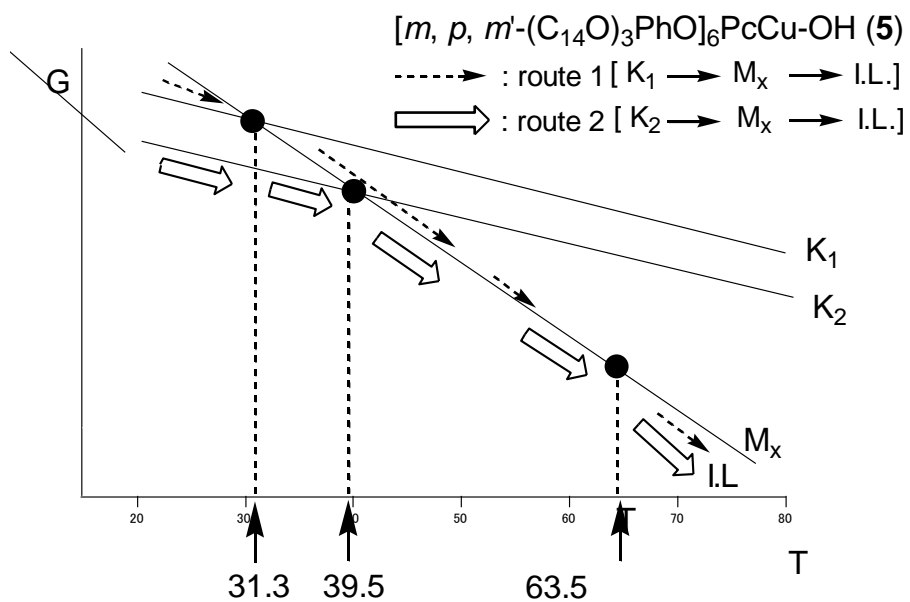
Figure 2. G-T diagrams of [*m, p, m'*-(C$_{14}$O)$_3$PhO]$_6$PcCu-OH (**5**), [*m, p, m'*-(C$_{14}$O)$_3$PhO]$_6$PcCu-OFBA (**6**) and [*m, p, m'*-(C$_{14}$O)$_3$PhO]$_6$PcCu-C$_{60}$ (**7**).
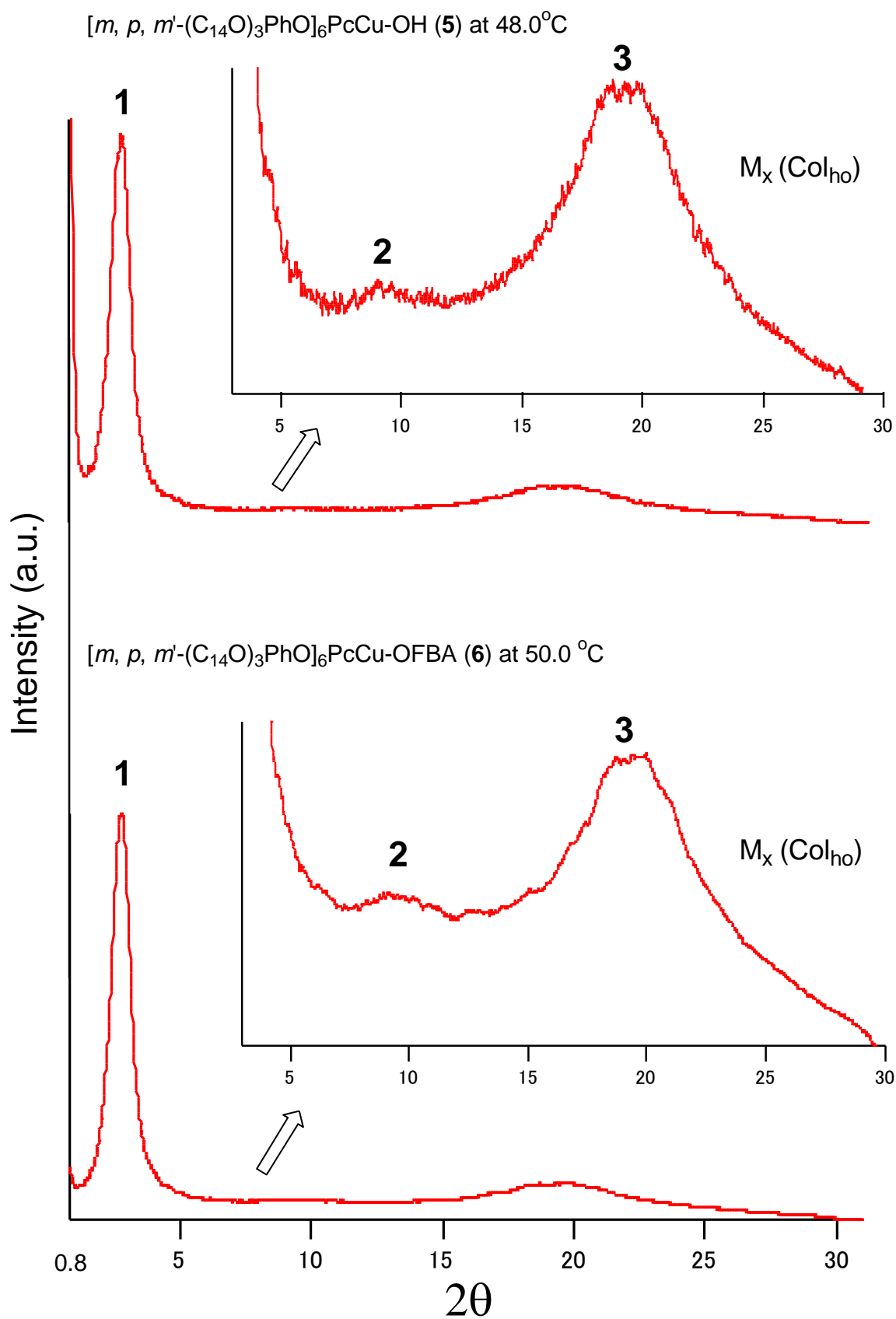
Figure 3. X-ray diffraction patterns of for [*m, p, m'*-(C$_{14}$O)$_3$PhO]$_6$PcCu-OH (**5**) at 48.0°C and [*m, p, m'*-(C$_{14}$O)$_3$PhO]$_6$PcCu-OFBA (**6**) at 50.0°C. *h* = stacking distance between the disks.
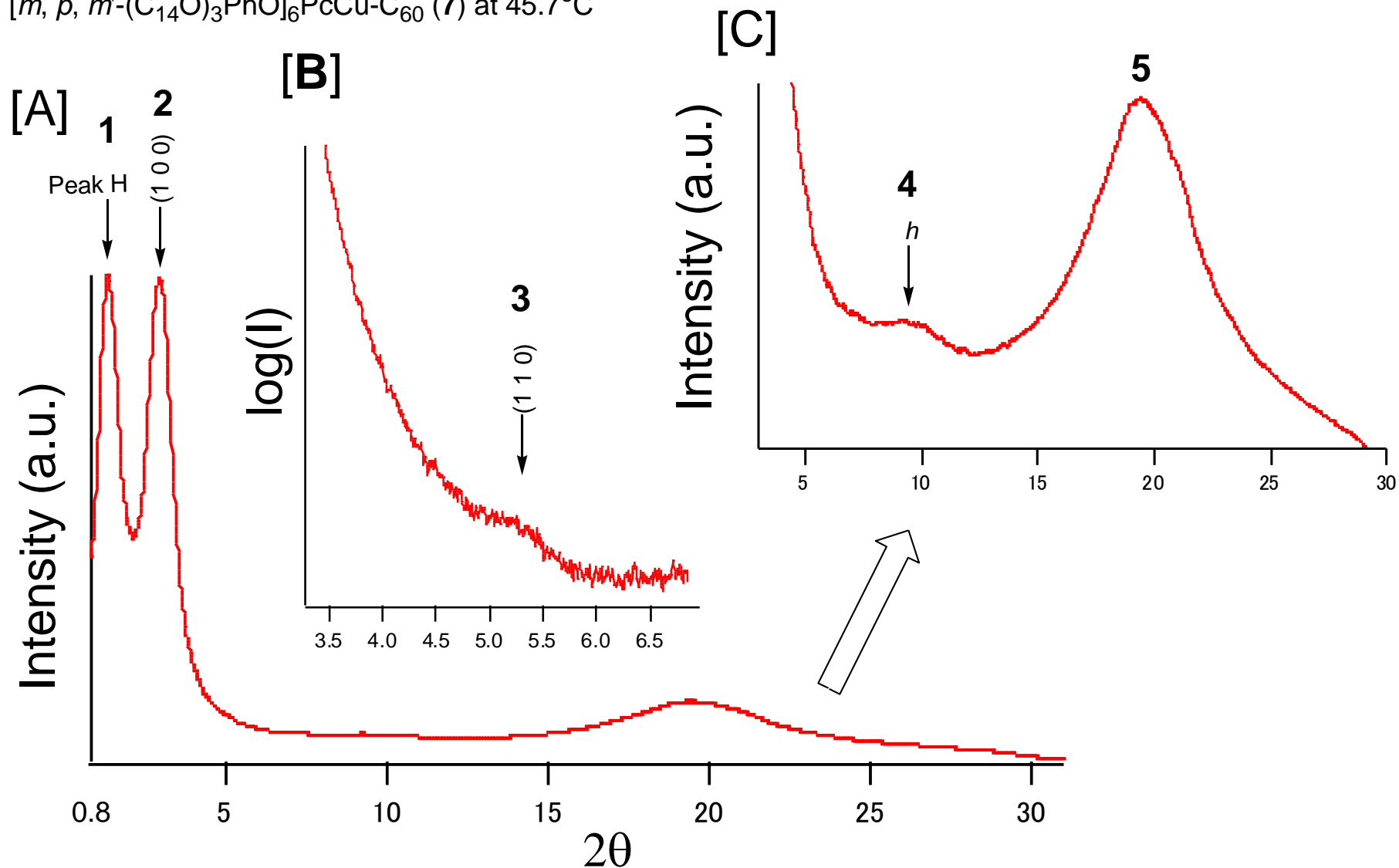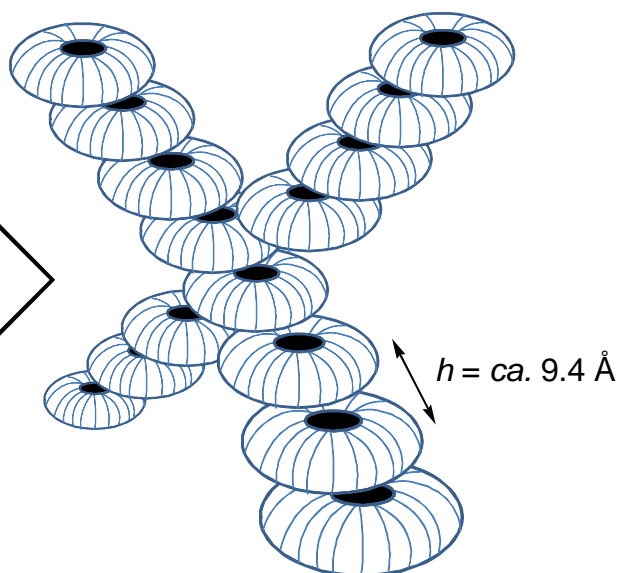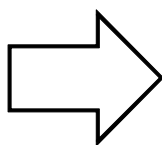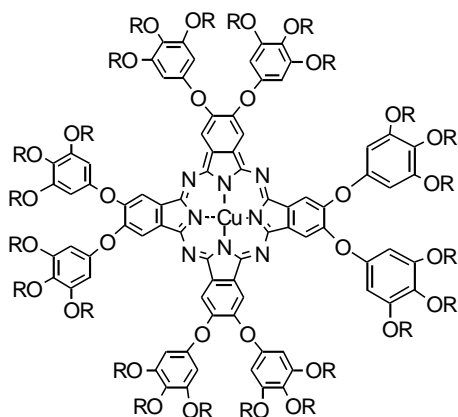
$[m, p, m'-(C_{14}O)_3PhO]_6PcCu-C_{60}$ (**7**) at 45.7^{o}C

[A] 1 2

Peak H

(1 0 0)

[B]

log(I)

3

(1 1 0)

[C] 5

4

h

Intensity (a.u.)

Intensity (a.u.)

Intensity (a.u.)

2θ

Figure 4. X-ray diffraction patterns of for $[m, p, m'-(C_{14}O)_3PhO]_6PcCu-C_{60}$ (**7**) at 45.7^{o}C. [A] and [C]: these patterns were obatined by using Bruker Mac SAXS system; [B]: this pattern was obatined by using Rigaku NANO-viewer SAXS system after annealing at 45.7^{o}C for 9 hours. h = stacking distance between the monomers and H = helical pitch of the fullerenes.

18

Table 6. X-ray data of [*m*, *p*, *m*'-(C$_{14}$O)$_3$PhO]$_6$PcCu-OH (**5**), [*m*, *p*, *m*'-(C$_{14}$O)$_3$PhO]$_6$PcCu-OFBA (**6**) and [*m*, *p*, *m*'-(C$_{14}$O)$_3$PhO]$_6$PcCu-C$_{60}$ (**7**).

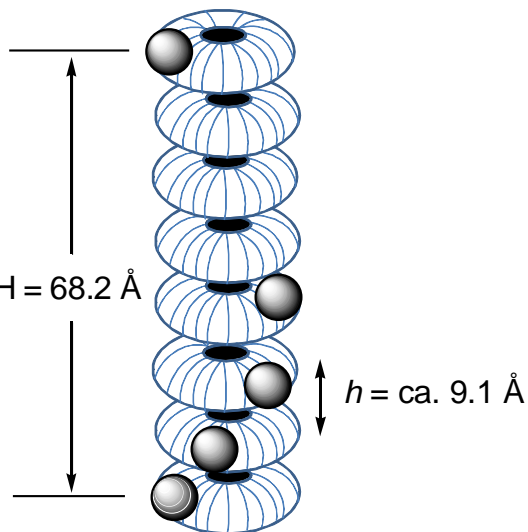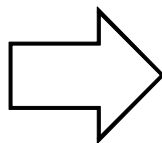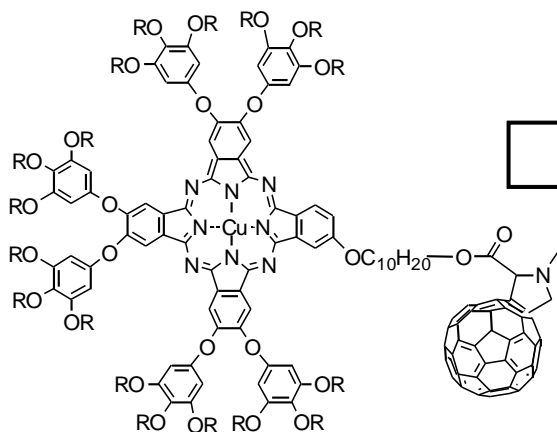| Compound	Mesophase Lattice constants(Å)	Peak No.	Spacing(Å) Observed	Spacing(Å) Calculated	Miller indices (h k l)
5: [*m*, *p*, *m*'-(C$_{14}$O)$_3$PhO]$_6$PcCu-OH	M$_x$ (Col$_{ho}$) at 48.0°C a = 37.8 h = ca.9.6 Z = 1.4 for ρ = 1.0	1 2 3	32.8 ca. 9.6 ca. 4.6	32.8 - -	(1 0 0) *h* *#*
6: [*m*, *p*, *m*'-(C$_{14}$O)$_3$PhO]$_6$PcCu-OFBA	M$_x$ (Col$_{ho}$) at 50.0°C a = 36.8 h = ca.9.4 Z = 1.3 for ρ = 1.0	1 2 3	31.9 ca. 9.4 ca. 4.6	31.9 - -	(1 0 0) *h* *#*
7: [*m*, *p*, *m*'-(C$_{14}$O)$_3$PhO]$_6$PcCu-C$_{60}$	Col$_{ho}$ at 45.7 °C a = 34.6 h = ca. 9.1 Z = 0.95 for ρ = 1.0	1 2 3 4 5	68.2 30.0 17.0 *ca.* 9.1 *ca.* 4.6	- 30.0 17.3 - -	H (1 0 0) (1 1 0) *h* *#*

h = Stacking distance between the monomers, H = Helical pitch of the fullerenes, # = Halo of the molten alkyl chains and ρ = assumed density (g/cm^3).

**Parent Pc compound [*m, p,*
m'-(C₁₄O)₃PhO]₈PcCu (4)**

$Cub(Pn\bar{3}m)$

$h = ca.$ 9.4 Å

**Child Pc-C₆₀ dyad [*m, p,*
m'-(C₁₄O)₃PhO]₆PcCu-C₆₀ (7)**

$H = 68.2$ Å

$h = ca.$ 9.1 Å

Col_{ho}

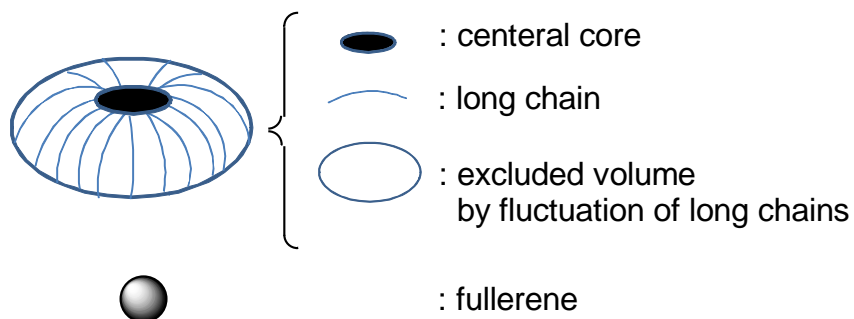: centeral core

: long chain

: excluded volume
  by fluctuation of long chains

: fullerene

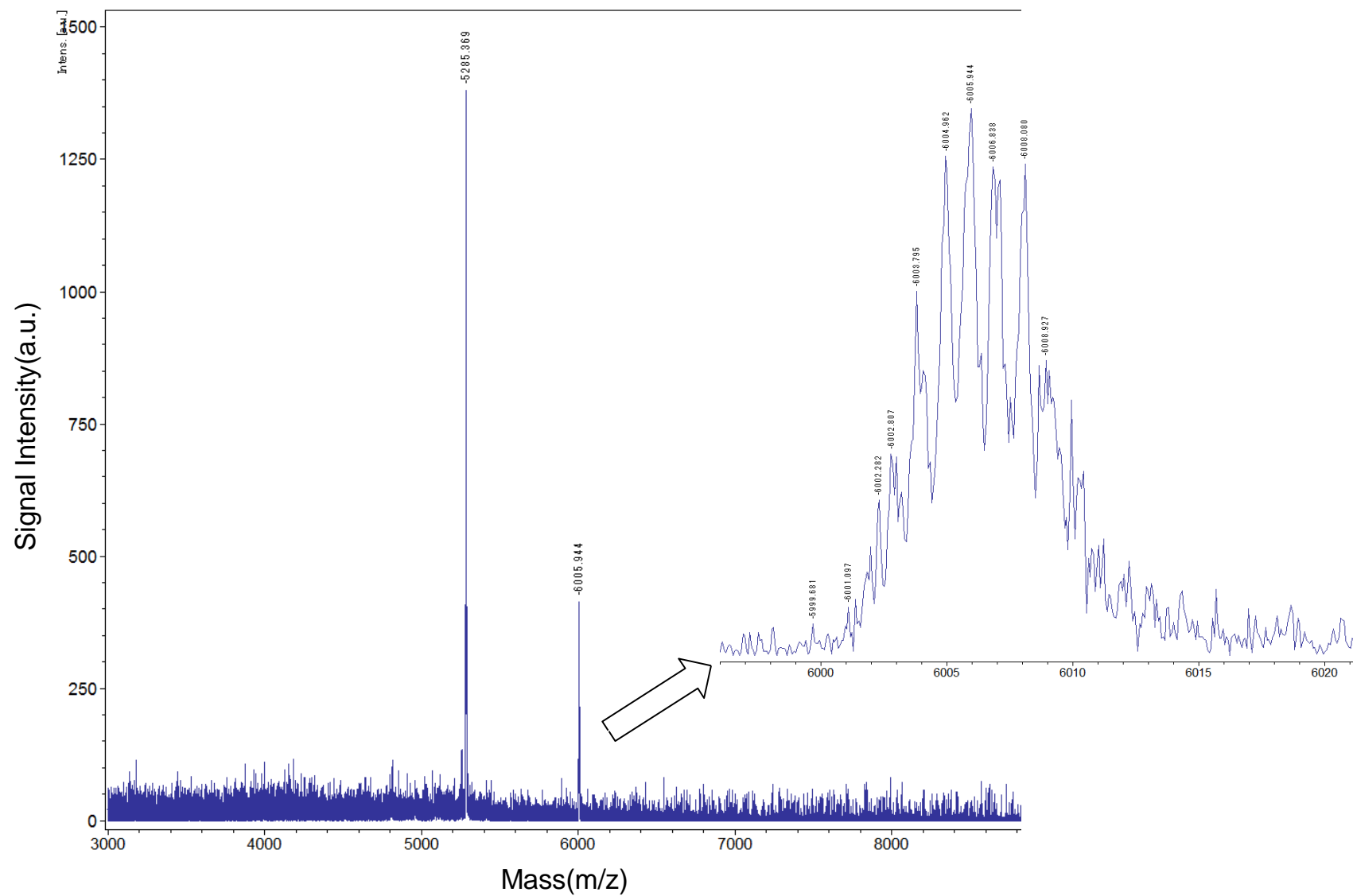Figure 5. Schematic illustration of the columnar structures of flat-pumpkin-shaped compounds **4** and **7**.

Figure S1. MALDI-TOFF mass spectra of the Pc-C_{60} dyad, [m, p, m'-($C_{14}O)_3$PhO]$_6$PcCu-C_{60} (**7**). The spectra were measured in positive ion reflector mode using 2, 5-dihydroxybenzoic acid as the matrix.